C–H···O Contacts in the Adenine···Uracil Watson–Crick and Uracil···Uracil Nucleic Acid Base Pairs: Nonempirical ab Initio Study with Inclusion of Electron Correlation Effects

ARTICLE *in* THE JOURNAL OF PHYSICAL CHEMISTRY B · JUNE 2000

Impact Factor: 3.3 · DOI: 10.1021/jp0007134

5 AUTHORS, INCLUDING:

Pavel Hobza
Academy of Sciences of the Czech Republic
317 PUBLICATIONS **18,095** CITATIONS
SEE PROFILE

Elena Cubero
31 PUBLICATIONS **1,155** CITATIONS
SEE PROFILE

C−H···O Contacts in the Adenine···Uracil Watson−Crick and Uracil···Uracil Nucleic Acid Base Pairs: Nonempirical ab Initio Study with Inclusion of Electron Correlation Effects

Pavel Hobza,*,† Jiří Šponer,† Elena Cubero,‡ Modesto Orozco,‡ and F. Javier Luque§

J. Heyrovský Institute of Physical Chemistry, Academy of Sciences of the Czech Republic, 182 23 Prague 8, Czech Republic, Departament de Bioquímica i Biologia Molecular, Facultat de Química, Universitat de Barcelona, Martí i Franqués 1, 08028 Barcelona, Spain, and Departament de Fisicoquímica, Facultat de Farmàcia, Universitat de Barcelona, Av. Diagonal s/n, 08028 Barcelona, Spain

Received: February 23, 2000

Structures and stabilities of H-bonded adenine···uracil Watson−Crick (AU WC) and two uracil···uracil nucleic acid base pairs possessing C−H···O contacts (UU7, UU−C) were determined using gradient optimization with inclusion of electron correlation via the second-order Møller−Plesset (MP2) perturbational method with a 6-31G** basis set of atomic orbitals. In the AU WC pair, closest contacts occur between the N6(A) and O4(U), N1(A) and N3(U), and C2(A) and O2(U) atoms: 2.969, 2.836, and 3.568 Å, respectively. For the UU7 pair the closest contact corresponds to O4···N1 and C5···O2 pairs with distances of 2.860 and 3.257 Å, respectively, while in UU−C pair the closest contact was found for O4···N3 and C5···O4 heteroatoms with distances of 2.913 and 3.236 Å, respectively. The nature of all intermolecular contacts in the sense of a conventional H-bonding or improper, blue-shifting H-bonding was determined on the basis of harmonic vibrational analysis, atom-in-molecules (AIM) Bader analysis of electron density, and natural bond orbital analysis (NBO) performed at the MP2/6-31G** level of theory. N−H stretch frequencies of A and U exhibited a red shift and intensity decrease upon formation of AU WC base pair. It unambiguously proves the existence of the N−H···O and O···H−N H-bonds. The frequency shift of the C−H stretching frequency of A upon complex formation is, however, marginal ($\sim$2 cm^{-1}). Bader AIM analysis and NBO analysis confirmed the existence of N−H···O and O···H−N H-bonds in the AU WC pair but was inconclusive in the case of C−H···O contact. The results thus clearly show that the C2−H2···O2 contact in the AU or AT WC base pair corresponds neither to standard H-bond nor to improper, blue-shifting H-bond. The opposite result, however, has been found for the UU pairs; here the vibrational analysis shows a red shift and intensity increase of both N−H and C−H stretching vibrational frequencies upon the formation of the pair. This is a clear manifestation of the presence of two H-bonds of the N−H···O and O···H−C types. Bader AIM analysis as well as NBO analysis confirmed the existence of both H-bonds.

1. Introduction

Hydrogen bonds (H-bonds) determine the three-dimensional structures of biomacromolecules and are therefore one of the key interactions in molecular biology. Most of the H-bonds are of X−H···Y types, where X is an electronegative atom and Y is either an electronegative atom with lone electron pair(s) or a region of excess of electron density. H-bonds where X and Y are F, O, or N atoms are well-known,[1,2] and the same is now true also for H-bonds with Y being aromatic π-electrons.[3−5] Already in 1982, a survey of crystal structures established the existence of C−H···O H-bonds[6] and extensive literature was devoted to this subject.[1,2,7] The C−H···O H-bonds are believed to be weak, and the question arises whether all C−H···O contacts correspond to standard H-bonds. Recently we suggested a new type of intermolecular bonding, termed improper, blue-shifting H-bonding,[8,9] with spectral manifestations quite opposite to those of H-bonding. (We called originally this bonding anti-H-bonding. This term was rightfully criticized as misleading mainly because it might contradict the existence of binding between both subsystems or it could evoke a complex with antihydrogen.) Instead of elongation of the X−H bond accompanied by a red shift of the X−H stretching frequency (typical for H-bonding), the improper, blue-shifting H-bonding is characteristic by contraction of the X−H bond and a blue shift of the respective X−H stretching frequency. The C−H···π improper, blue-shifting H-bonding was theoretically predicted and later detected by double-resonance ion-depletion infrared spectroscopy.[9] Theoretical prediction was based on geometrical characteristics obtained from standard and counterpoise (CP)-corrected geometry optimizations and vibrational frequencies determined by harmonic and anharmonic vibrational analysis. Analysis of the electron density topology obtained from atom-in-molecules (AIM) Bader theory[10] suggests that the specific features of the improper H-bonds originates from redistribution of electron density in the C−H bond induced upon complexation.[11] Specifically, the electron density at the bond critical point (bcp) increased if an improper H-bond is formed while it decreased if a standard H-bond is formed.[11] The family of improper, blue-shifting H-bonds was recently extended to improper H-bonds of the C−H···O type, and the C−H···O improper H-bond in fluoroform···ethylene oxide[12] was manifested by 0.1

* Corresponding author. Fax: 420 2 858 2307. E-mail: hobza@indy.jh-inst.cas.cz.
† Academy of Sciences of the Czech Republic.
‡ Facultat de Quimica, Universitat de Barcelona.
§ Facultat de Farmàcia, Universitat de Barcelona.

10.1021/jp0007134 CCC: $19.00
Published on Web 06/10/2000

pm contraction of C−H bond and significant (∼30 cm^{-1}) blue shift of the C−H stretching frequency accompanied by lowering of intensity of the respective vibration. Also in this case the Bader AIM theory predicted[13] an increase in the C−H electron density induced upon complexation which justifies the shortening of the C−H bond and the respective blue shift in the C−H stretch frequency.

A very large blue shift of the C−H stretch frequency, more than 100 cm^{-1}, was detected recently from infrared spectra of $X^-\cdots H_3CY$ ionic complexes (X = Cl, Y = Br; X, Y = I), which were also thoroughly investigated theoretically.[14] Contrary to the halogen substituents, for Y = H, methane displays a red shift upon complexation with both anions. The natural bond orbital (NBO) analysis was used[14] for explaining the different origin of bonding in these ion−molecule complexes. It was demonstrated that formation of H-bonds in $X^-\cdots$methane complexes is accompanied by electron density transfer (EDT) from halide anion lone pairs to the C−H σ^* antibonding orbitals. Formation of improper H-bonds in the $X^-\cdots H_3CY$ complexes is accompanied, on the other hand, with an EDT to C−Y σ^* antibonding orbital. Let us finally mention that the EDT concept of H-bonding using NBO analysis was introduced by Reed, Curtiss, and Weinhold.[15]

X−H···Y H-bonds with X and Y being N and O are well-known in nucleic acid base pairing and contribute significantly to the stability of a pair. The C−H···O contacts in nucleic acid base pairs are less frequent and mostly exist as base−backbone contacts between purine C8−H or pyrimidine C6−H and the O5′ atom in the backbone[16] when the bases are in the anti-conformation. There are, however, also C−H···O base−base contacts. Such contacts occur also in AT/U WC or Hoogsteen pairs. Conventionally, the AT/U WC pair which exist in the crystal of DNA/RNA is linked by two H-bonds of the N−H···O and N···H−N type which correspond to close N···O and N···N contacts. Hunter and co-workers[17] speculated recently that the third long C···O contact in the AU WC pair might correspond to a third H-bond which would contribute to the stability of the pair. This idea was supported by Starikov and Steiner;[18] they considered this interaction "*cum grano salis* as a weak H-bond." Another example of the C−H···O contact was found recently in the uracil···uracil base pair, referred to as the Calcutta pair. The Calcutta pair discovered in the crystal structure of RNA[16] was believed to have a conventional N3−H···O4 and an unconventional C5−H···O4 H-bond.

Recently, the potential energy surface of isolated uracil dimer in the gas phase was investigated[19] in our laboratory using molecular dynamics/quenching techniques and ab initio calculations. The simulations revealed that the Calcutta pair (designated UU−C) is not significantly populated in the gas phase, since its stabilization energy is rather low. However, another structure (designated as UU7) with the C−H···O contact was found to be quite populated. Besides the C−H···O contact, the structure was stabilized by an N1−H···O H-bond; this H-bond is considerably stronger than N−H···O bonds involving N3 atom. However, the UU7 pair cannot occur in nucleic acids since the N1 position is not accessible to H-bonding. Because both UU7 and UU−C pairs are important, we included both of them in the present analysis.

The aim of the study is clarify the nature of C−H···O contacts occurring in the AU WC, UU−C, and UU7 base pairs and specify whether they correspond to H-bonds, improper H-bonds, or other types of interactions. Among other calculations we report the first MP2 vibrational analysis of DNA base pairs, supplemented by Bader analysis of the electron densities and NBO analysis. Both analyses were performed at the correlated MP2 level. The calculations clearly identify the existence of the C−H···O H-bond in the UU base pairs while we have found no justification to speculate about a third H-bond in AU and AT WC base pairs.

2. Calculations

The geometries of AU WC and UU pairs and monomers were optimized at the Hartree−Fock (HF) level using the 6-31G** basis set[20] and at correlated second-order Møller−Plesset level (MP2) with the same basis set. The frozen core approximation was adopted in MP2 calculations. No symmetry constraint was considered in the optimization. The final stabilization energy for the optimized complex was determined by correcting for the basis set extension effects, which were eliminated using the Boys−Bernardi counterpoise method.[21] Further, the deformation energies of bases upon complexation were subtracted; these were calculated as the difference of the energies of the optimized bases and the energies of bases with the same geometry as within the complex. It means that structure of a complex was optimized at a standard potential energy surface (PES), i.e., without counterpoise corrections and not at the theoretically more justified CP-corrected PES. The structure of the AT WC pair was therefore re-optimized by the CP-corrected gradient optimization[22] at the HF/6-31G** level, to show that the explicit inclusion of BSSE in the course of the optimization does not change the results qualitatively. In CP-corrected optimizations the basis set superposition error is eliminated in each gradient cycle. Harmonic vibrational frequencies were determined using Wilson's FG analysis. We have shown previously[23] that harmonic intermolecular vibrational frequencies of the AT WC pair agree well with the corresponding anharmonic frequencies. All the calculations were performed with the GAUSSIAN 94[24] and GAUSSIAN 98[25] codes.

The electron density topological analysis was carried out using the theory of atoms in molecules,[10] which has been successfully used to characterize H-bonds in a variety of molecular complexes.[26] Calculations were performed using the molecular structures optimized at the MP2 level. Attention was focused on the properties of the (3,−1) bond critical points and on selected integrated atomic properties of the hydrogen atoms participating in H-bond interactions. Calculations were conducted with the program PROAIM.[27]

3. Results and Discussion

3.1. Geometries, Energies, and Vibrational Analysis. Structures and atom numbering of optimized AU WC, UU7, and UU−C base pairs are shown in Figure 1, and the respective geometrical, vibrational, and energetical characteristics are presented in Table 1.

The MP2 stabilization energies for both pairs are larger than the HF values, because the MP2 method includes the dispersion energy neglected within the HF approximation. Note that the UU7 base pair is considerably more stable than the UU−C one and is at least partly competitive with those UU pairs which are stabilized by two N−H···O H-bonds.[19] Thus the pair is expected to be detectable in gas-phase experiments, in contrast to UU−C.[19]

The intersystem distances obtained at the MP2 optimization are shorter than the HF ones, consistent with MP2 optimizations reported earlier for selected pyrimidine base pairs.[28] The reason is obviously the neglect of dispersion attraction by the HF method. Let us first discuss the more accurate MP2 characteristics. Analyzing the non-hydrogen atom distances in the AU

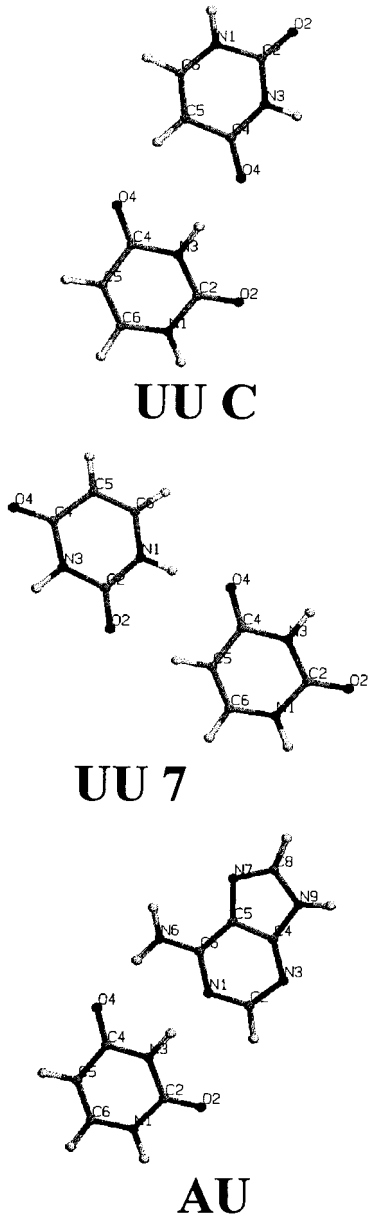

Figure 1. Structures and atom numbering of AU WC, UU7, and UU−C base pairs.

WC pair, we found that the C2−O2 distance (3.57 Å) is considerably longer than the N6−O4 and N1−N3 distances (2.97 and 2.84 Å). Further, the C2−H2 covalent bond length is practically unchanged upon complex formation while the N6−H6 bond and especially N3−H3 bond are significantly elongated. The calculated shifts in X−H stretching vibration frequencies upon the formation of the complex agree with the geometrical results. The largest red shift was found for the N3−H3 stretching frequency of uracil (618 cm^{-1}). Also the N6−H6 amino stretching vibration frequency of adenine shows a large, though considerably smaller red shift upon the formation of the base pair (145 cm^{-1}) while the C2−H2 stretching frequency of adenine is practically unchanged by the complex formation. All these data are consistent with the existence of strong N3−H3···N1 and moderate N6−H6···O4 H-bonds. There is, however, no evidence of formation of either an H-bond or improper H-bond in the case of C2−H2···O2 contacts. The HF results agree basically with the MP2 values giving evidence about the dominant role of electrostatic interaction. The relative changes of distances and vibrational frequencies are at the HF level consistently smaller since the base pair strength is undervaluated.

The role of CP-corrected optimization was studied for the AT WC pair. We performed standard and CP-corrected HF/6-31G** gradient optimization for this pair and found that in both cases optimization led to a planar structure. The CP-corrected optimization resulted in slightly larger intermolecular separations: N1−N3 and N6−O4 distances increased by 0.055 and 0.005 Å, respectively. The changes of N6−H6, N3−H3, and C2−H2 bonds upon complex formation remain, however, the same as in standard gradient optimization. It indicates that the basis set extension artifact does not influence the results substantially.

The situation with the UU7 base pair is different. The C5−O2 distance (3.26 Å) is again longer than that of O4−N1 (2.86 Å), but the C···O contact is considerably shorter than that in the AU WC pair. Also other geometrical and vibrational data are consistent with the existence of two H-bonds of the N1−H1···O4 and C5−H5···O2 type. The former H-bond is stronger than the N6−H6···O4 H-bond in the AU WC pair and is characterized by a red shift of 288 cm^{-1}. The red shifts of symmetrical and antisymmetrical C5−H5 stretching frequencies are considerably smaller (34 and 5 cm^{-1}) but clearly supporting the existence of a C−H···O H-bond. It should be mentioned that at the HF level we obtained for these frequencies red and blue shifts of 32 and 23 cm^{-1}, respectively. It shows that for a quantitative analysis of base pairing the electron correlation should be included. The C5−O4 and O4−N3 distances (3.24 and 2.91 Å) in UU−C are similar to those in the UU7, and these contacts are consistent with the existence of two H-bonds of the C5−H···O4 and N3−H···O4 type. They are characterized by elongation of N3−H and C5−H bonds by 0.014 and 0.002 Å what is similar to those found in N−H···N and C−H···O bonds in UU7. For the UU−C we did not performed the MP2 harmonic vibrational analysis.

3.2. Electron Density Topological Analysis. *AU WC Base Pair*. The formation of the AU WC complex gives rise to the appearance of five critical points (see Figure 2). Three are (3,−1) critical points linking the atoms H6(A) and O4(U), N1-(A) and H3(U), and H2(A) and O2(U). The other two are (3,+1) critical points appearing between the bond critical points. Table 2 gives the topological properties of the (3,−1) critical points formed upon dimerization. The electron density at the bond critical points varies from 0.0059 to 0.0434 au. These values are within the range determined for similar H-bonded complexes, which typically varies from 0.002 to 0.04 au.[26a,29] The value for the H2···O2 interaction (0.0059 au) is sensibly lower than that for the H6···O4 (0.0251 au) and N1···H3 (0.0434 au) interactions, in agreement with the differences in geometrical distances for the intermolecular contacts (see above and Table 1). As expected for closed-shell interactions, the Laplacian of the electron density is positive, which indicates a depletion of electron density from the interatomic surface toward the interacting nuclei, as noted in the positive value of λ_3, which is much larger than the other two eigenvalues.

An additional indication of the strength of the intermolecular contacts comes from comparison of the penetration effects between the H-bond acceptor and hydrogen atoms, which can be measured from the difference between atomic radii for the bonded and nonbonded monomers. In the bonded complex the atomic radius is determined as the distance to the intermolecular bond critical point from the atom, and in the isolated monomer it is estimated as the distance from the atom to an isodensity

TABLE 1: Stabilization Energies[a] (ΔE), Intermolecular X−Y Distances[b] (r), and Changes of X−H Distances[b] (Δr) and Vibration Stretching Frequencies[c] ($\Delta\nu$) upon Formation of a Complex in the AU WC, UU7, and UU−C Pairs Determined at the HF/6-31G and MP2/6-31G** Levels**

complex[d]	level	ΔE	$r(N_6-O_4)$	$\Delta r/\Delta\nu(N_6-H_6)$	$r(N_1-N_3)$	$\Delta r/\Delta\nu(N_3-H_3)$	$r(C_2-O_2)$	$\Delta r/\Delta\nu(C_2-H_2)$
AU WC	HF	9.8	3.083	0.007/−43[e], −84[f]	2.989	0.016/−320	3.780	0/+9
	MP2	12.1	2.969	0.009/−32[e], −145[f]	2.836	0.045/−618	3.568	0/−2

complex[d]	level	ΔE	$r(O_4-N_1)$	$\Delta r/\Delta\nu(N_1-H_1)$	$r(C_5-O_2)$	$\Delta r/\Delta\nu(C_5-H_5)$
UU7	HF	9.9	2.946	0.010/−179	3.398	0.002/ +23[e], −32[f]
	MP2	11.5	2.860	0.016/−288	3.257	0.003/−5[e], −34[f]

complex[d]	level	ΔE	$r(O_4-N_3)$	$\Delta r(N_3-H_3)$	$r(C_5-O_4)$	$\Delta r(C_5-H_5)$
UU−C	MP2	8.1	2.913	0.014	3.236	0.002

[a] Energies in kcal/mol. [b] Distances in Å. [c] Vibration frequencies in cm^{-1}. [d] Cf. Figure 1. [e] Antisymmetrical vibration. [f] Symmetrical vibration.

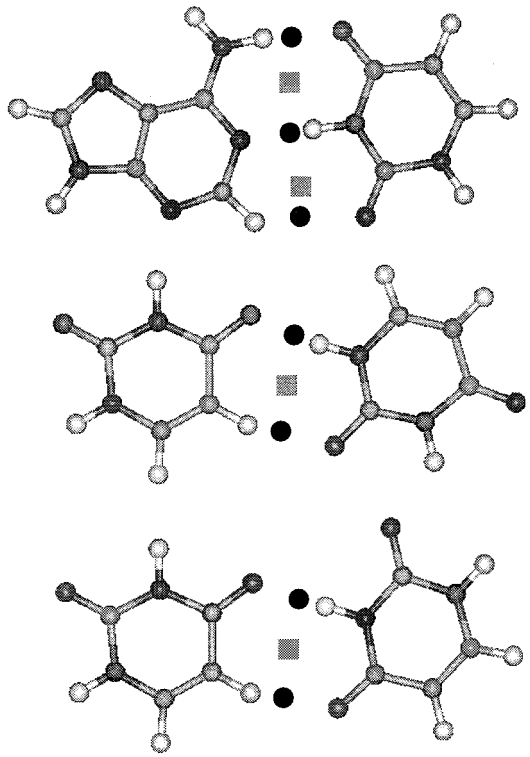

Figure 2. Representation of the bond (circle) and ring (square) critical points formed in the adenine−uracil (top) complex and in the two uracil (UU7, middle; UU−C, bottom) dimers.

contour (a value of 0.001 au has been adopted here) in the direction of the hydrogen bond. The results in Table 2 indicate a mutual penetration of the interacting H-bond acceptor and hydrogen atoms varying between 1.0 and 1.3 Å for the N6−H6···O4 and N3−H3···N1 contacts. Nevertheless, this effect is clearly less important for the C2−H2···O2 contact, which agrees with the largest interatomic distance (see Table 1).

Table 2 also gives the topological properties for the (3,−1) critical points of the N−H and C−H bonds involved in hydrogen-bond interactions in the dimer, as well as in the isolated monomers. The values of the electron density at these critical points are larger by roughly 1 order of magnitude than the electron densities of the intermolecular (3,−1) critical points, as expected from the covalent nature of the bonds. The dimerization decreases the electron density at the intramolecular (3,−1) critical point of N6−H6 and N3−H3 bonds by around 0.012 and 0.032 au, as occurs for conventional hydrogen bonds. Nevertheless, the electron density in the C2−H2 bond remains nearly unaffected.

According to Popelier's criteria for hydrogen bonding,[26] the hydrogen atoms involved in hydrogen bonding exhibit similar changes in selected integrated atomic properties, which are (i) an increase in the net charge, (ii) a lowering in the in the absolute value of the atomic energy, (iii) a reduction in the first moment, and finally (iv) a decrease in the atomic volume. All these trends are found for the hydrogen atoms in the X−H bonds that participate in intermolecular interactions, as can be seen from inspection of Table 3. For the N−H bonds, the net charge is increased by around 0.009 units of electron, the atomic energy decreases in absolute value by 0.05 au, the first moment is reduced by around 0.04 au, and the atomic volume is diminished by around 11 au. These changes are significantly less marked for the hydrogen atom of the C2−H2 bond.

UU Pairs. The formation of the two uracil dimers gives rise to the appearance of three critical points (see Figure 2). Two are (3,−1) bond critical points between atoms O4···H1 and H5···O2 in UU7 and O4···H3 and H5···O4 in UU−C, and the other is a ring critical point located between the two intermolecular (3,−1) critical points. The topological properties of the electron density at the (3,−1) critical points in O4···H1 (UU7) and O4···H3 (UU−C), as well as in H5···O2 (UU7) and H5···O4 (UU−C), are very similar (Table 4), despite the different stabilization energy of the corresponding complexes (see Table 1).

The electron density at the (3,−1) critical points (Table 4) lies within the expected range for similar interactions.[26a,29] They are, however, larger than the values found for the H6···O4 and H2···O2 bonds in the AU WC pair (see Table 1). Indeed, the mutual penetration of the hydrogen-bond acceptor and hydrogen atoms (Table 3) is slightly larger for the UU pairs than for the corresponding contacts in the AU dimer. This effect is particularly relevant in the H5···O2 (UU7) and H5···O4 (UU−C) bonds compared to the H2···O2 contact (AU), since the mutual penetration in the two former cases is around 0.4 Å larger than for the corresponding contact in AU. The electron density at the N1−H1 (UU7) and N3−H3 (UU−C) bonds is reduced upon dimerization by ∼0.016 au, and the electron density at the C5−H5 bond is increased by ∼0.002 au. These changes are larger than the corresponding variations observed for the N6−H6 and C2−H2 bonds in the AU pair.

Table 5 shows the changes in the integrated atomic properties for the hydrogen atoms involved in hydrogen bonding for the UU pairs. Again, all the changes follow the expected trends pointed out by Popelier.[26] Importantly, the changes experienced by the hydrogen atom in the C5−H5 bond are sensibly larger than those found for the hydrogen atom in the C2−H2 bond in the AU dimer (see Table 3).

Bond Order−Bond Length Relationships. The dependence between the intermolecular distance and the logarithm of the

TABLE 2: Electron Density Topological Properties[a] at the (3,−1) Critical Points for the X−H···Y Contacts Formed upon Complexation between Adenine and Uracil and at the (3,−1) Critical Points of the Participating X−H Bonds in the Dimer and in the Isolated Monomers

bond	ρ	$\nabla^2\rho$	λ_1	λ_2	λ_3	Δr_H	Δr_Y	$\Delta r_H + \Delta r_Y$
			AU WC Intermolecular Bonds					
H6···O4	0.0251	0.0710	−0.0321	−0.0315	0.1346	0.503	0.503	1.006
N1···H3	0.0434	0.1003	−0.0673	−0.0641	0.2317	0.609	0.714	1.323
H2···O2	0.0059	0.0214	−0.0055	−0.0052	0.0321	0.265	0.132	0.397
			AU WC Intramolecular Bonds					
N6−H6	0.3305	−1.7893	−1.3580	−1.2993	0.8679			
N3−H3	0.3075	−1.6375	−1.2771	−1.2371	0.8768			
C2−H2	0.2956	−1.1564	−0.8339	−0.7961	0.4737			
			A Bonds					
N6−H6	0.3426	−1.8228	−1.3270	−1.2612	0.7655			
C2−H2	0.2942	−1.1309	−0.8216	−0.7823	0.4730			
			U Bonds					
N3−H3	0.3394	−1.8288	−1.3395	−1.2842	0.7949			

[a] Properties are electron density (ρ) and its Laplacian ($\nabla^2\rho$) and eigenvalues (λ); penetration effects are determined from the difference between nonbonded and bonded radii (Δr).

TABLE 3: Integrated Atomic Properties[a] for the Hydrogen Atoms in the X−H Bonds Involved in Hydrogen Bonding in the Adenine−Uracil Pair and in the Respective Isolated Monomers with the Change for a Given Property in the Dimer Relative to the Isolated Monomer Given in Parentheses

atoms	q	E	$\|M\|$	V
		AU WC Bonds		
(N6)H6	0.530 (+0.090)	−0.3894 (+0.0504)	0.133 (−0.043)	17.67 (−10.13)
(N3)H3	0.555 (+0.086)	−0.3670 (+0.0560)	0.118 (−0.048)	14.54 (−12.11)
(C2)H2	0.058 (+0.037)	−0.6185 (+0.0158)	0.113 (−0.013)	44.52 (−3.15)
		A Bonds		
(N6)H6	0.441	−0.4398	0.176	27.80
(C2)H2	0.021	−0.6343	0.126	47.67
		U Bonds		
(N3)H3	0.469	−0.4230	0.166	26.65

[a] All values in atomic units: q, net charge; E, energy; M, first moment; V, volume.

TABLE 4: Electron Density Topological Properties[a] at the (3,−1) Critical Points for the X−H···Y Contacts Formed upon Formation of the Two Uracil Dimers and at the (3,−1) Critical Points of the Participating X−H Bonds in the Dimer and in the Isolated Monomers

bond	ρ	$\nabla^2\rho$	λ_1	λ_2	λ_3	Δr_H	Δr_Y	$\Delta r_H + \Delta r_Y$
			UU7 Intermolecular Bonds					
O4···H1	0.0323	0.0956	−0.0455	−0.0442	0.1853	0.556	0.556	1.112
H5···O2	0.0164	0.0467	−0.0182	−0.0182	0.0831	0.477	0.397	0.874
			W7 Intramolecular Bonds					
N1−H1	0.3269	−1.7757	−1.3580	−1.3085	0.8908			
C5−H5	0.2892	−1.1228	−0.7973	−0.7755	0.4500			
			UU−C Intermolecular Bonds					
O4···H3	0.0285	0.0841	−0.0385	−0.0377	0.1602	0.535	0.533	1.068
H5···O4	0.0166	0.0477	−0.0186	−0.0184	0.0847	0.475	0.401	0.876
			W−C Intramolecular Bonds					
N3−H3	0.3244	−1.7632	−1.3391	−1.2934	0.8693			
C5−H5	0.2896	−1.1247	−0.7984	−0.7767	0.4504			
			U Bonds					
N1−H1	0.3431	−1.8486	−1.3560	−1.2948	0.8022			
N3−H3	0.3394	−1.8288	−1.3395	−1.2842	0.7949			
C5−H5	0.2874	−1.0690	−0.7720	−0.7476	0.4506			

[a] See footnote in Table 2.

electron density at the bond critical point, which can be used as a measure of the bond order,[30] is given in Figure 3 for the seven intermolecular bond critical bonds in the AU and UU pairs. Inspection of Figure 3 shows the existence of a linear relationship between the interatomic H···X distance (d) and the logarithm of the electron density (ρ) ($d = 0.16-0.50 \ln \rho$; $r = 0.99$), which agrees with previous bond order−bond length relationship studies in similar H-bonded complexes.[11,26g,29,30,31]

Comparison of the changes in bond lengths and vibrational stretching frequencies for the X−H bonds upon complexation in the AU and UU pairs is made in Figure 4. There is a relationship between the change in the electron density at the (3,−1) critical point of the X−H bond and the variation in either the bond length or the vibrational frequency. Nevertheless, there is a subtle difference in the behavior observed for N−H and C−H bonds. In the former case, there is a depletion in the electron density at the N−H bond critical point upon complexation (see Tables 2 and 3), which is larger as the interatomic distance becomes smaller: this effect decreases in the order N3−H3 (AU) > N1−H1 (UU7) > N3−H3 (UU−C) >

TABLE 5: Integrated Atomic Properties[a] for the Hydrogen Atoms in the X−H Bonds Involved in Hydrogen Bonding in the Two Uracil Dimers and in the Respective Isolated Monomers with the Change for a Given Property in the Dimer Relative to the Isolated Monomer Given Parentheses

atoms	*q*	*E*	|*M*|	*V*
		UU7 Bonds		
(N1)H1	0.544 (+0.078)	−0.3833 (+0.0442)	0.123 (−0.043)	16.05 (−10.45)
(C5)H5	0.130 (+0.083)	−0.5797 (+0.0331)	0.091 (−0.031)	36.86 (−9.49)
		UU−C Bonds		
(N3)H3	0.543 (+0.074)	−0.3813 (+0.0417)	0.125 (−0.041)	16.64 (−10.01)
(C5)H5	0.128 (+0.081)	−0.5813 (+0.0315)	0.092 (−0.030)	36.97 (−9.38)
		Uracil Bonds		
(N1)H1	0.467	−0.4275	0.166	26.50
(N3)H3	0.469	−0.4230	0.166	26.65
(C5)H5	0.047	−0.6128	0.122	46.35

[a] See footnote in Table 3.

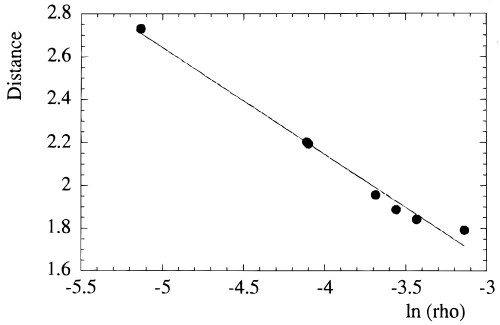

Figure 3. Representation of the change in the interatomic H···X distance (Å) vs the variation in the logarithm of the electron density at the corresponding bond critical point for the adenine−uracil complex and the two uracil dimers.

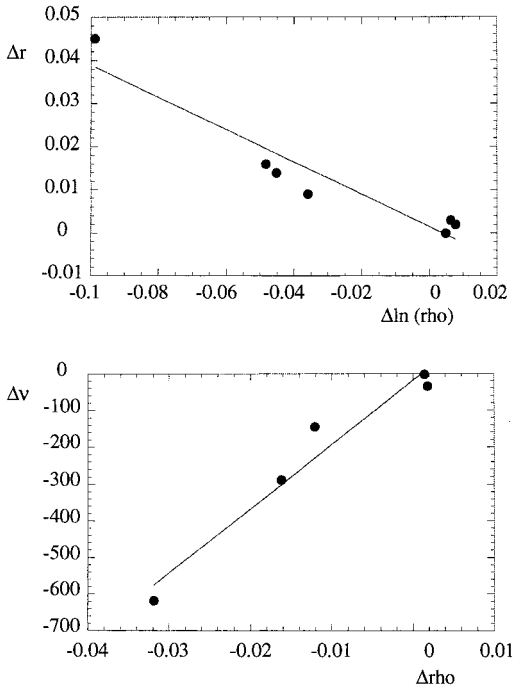

Figure 4. Representation of (top) the change in the bond length of the X−H bonds (Δ*r*; Å) involved in intermolecular contacts vs the variation in the logarithm of the electron density and (bottom) the stretching frequency shift (cm^{-1}) vs the variation in the electron density (ua) at the corresponding bond critical points.

N6−H6 (AU). Indeed, the largest the electron density depletion, the greatest the changes experienced in bond length and red shift. However, in C−H bonds there is an increase in the electron density upon complexation, and this effect is larger as the interatomic distance becomes shorter (the magnitude of this effect decrease in the order C5−H5 (UU7) ∼ C5−H5 (UU−C) > C2−H2 (AU)). This different behavior likely stems from the different nature of stabilizing forces in intermolecular contacts involving N−H or C−H bonds, since the former are expected to be dominated by electrostatics, whereas dispersion is more important in the latter.

For our purposes here, the preceding results suggests that the C−H···O contacts in AU and UU pairs exert different contributions to the stabilization of the corresponding complexes. Thus, the C2−H2···O2 bond in the AU pair is expected to be sensibly less stabilizing than the C5−H5···O2 and C5−H5···O4 bonds in the UU pairs. Indeed, the changes in the integrated atomic properties of the hydrogen atom in the C2−H2 bond in the AU pair are clearly smaller than those observed for the hydrogen atoms of the C5−H5 bonds in the UU dimers. Overall, whereas the C5−H5···O hydrogen bond contributes to the formation of the uracil dimers, the results allow us to argue against a significant role of the C2−H2···O2 contact in stabilizing the AU WC pair.

3.3. Natural Bond Orbital Analysis. *AU WC Base Pair.* Analyzing the NBO densitites, we found an electron density transfer (EDT) of 318 me from adenine to uracil. Investigating individual densities, we found the largest EDT from the adenine N1 lone electron pairs to the thymine N3−H3 σ^* antibonding orbital (649 me) and from the thymine O4 lone electron pairs to the adenine N6−H61 σ^* antibonding orbital (265 me). Summing these two EDTs, one obtains an EDT of 384 me from adenine to thymine what is close to the total EDT of 318 me. In both cases we obtain an electron density increase in the X−H σ^* antibonding orbitals which results in weakening of these bonds, their elongation, and a concomitant red shift of their strech frequencies. Evidently, N1···H3−N3 as well as O4···H61−N6 contacts correspond to standard H-bonding. The situation is different in the case of the O2···H2−C2 contact. The electron density in the adenine C2−H2 σ^* antibonding orbital is not changed upon formation of a pair which excludes formation of the respective H-bond as well as improper H-bond. This is also supported by the net change of the thymine O2 natural charge that becomes slightly more negative upon formation of a pair. Let us recall that existence of an H-bond as well as an improper H-bond of the X−H···Y type is connected with electron density decrease at the proton acceptor (Y).

UU Pairs. From the NBO densities of UU7 pair it follows that electron density is transferred from the uracil acting as C−H proton donor to the other one. The total EDT (287 me) is slightly smaller than that in AU WC. Analyzing the electron densities in the N−H···O contact, we found electron density decrease at the O4 lone electron pairs and a large electron density increase

(38 me) in the N1−H1 σ^* antibonding orbital. In the case of the C−H...O contact we detected again an electron density increase (13 me) in the C5−H5 σ^* antibonding orbital, but here electron density at the O2 lone electron pairs slightly increases (by 2 me). Electron density increase in N1−H1 and C5−H5 σ^* antibonding orbitals leads to weakening of both bonds, their elongation, and a concomitant red shift of the respective strech vibration frequencies. Though the EDT to C5−H5 antibonding orbital is smaller than that to N1−H1, this gives clear evidence about formation of the standard (though weak) H-bond of the C−H···O type. The situation in the UU−C pair is similar. Also here we found a rather strong N1−H···O4 H-bond characteristic by increase of electron density in the N1−H σ^* antibonding orbital (33 me) which is accompanied by the N1−H bond length increase. The C5−H···O2 contact corresponds also to an H-bond, which is, however, weaker. The electron density in the σ* antibonding orbital increases by 12 me which is accompanied by bond length increase.

4. Conclusion

Harmonic vibrational analysis performed at the correlated MP2 level reveals two H-bonds of N−H···N and N−H···O types in the AU WC base pairs while no support is given to existence of the third bond, either C−H···O H-bond or improper, blue-shifting H-bond. The H2 adenine hydrogen does not play any active role in the pairing. On the other hand, the vibrational analysis shows two H-bonds of N−H···O and C−H···O types in the UU7 base pair. Vibrational analysis results agreed with atom-in-molecule Bader analysis of electron density and with natural bond orbital analysis. It is thus possible to conclude that there are two strong H-bonds in the AU WC pair and one strong and one weaker H-bonds in both UU pairs. The existence of the third H-bond in the AU pair was ruled out, which fully agrees with recently published results obtained using HF and density functional theory methods.[32]

Acknowledgment. We thank Prof. R. W. F. Bader for sending us a copy of the PROAIM computer program. This study was supported by Grants 203/98/1166 and 203/00/0633 from the Grant Agency of the Czech Republic and by Grants PB98-1222 and PB96-1005 from the Spanish DGICYT. We also thank the Centre de Supercomputació de Catalunya (CESCA; Molecular Recognition project) and the Supercomputer Center, Brno, Czech Republic, for computational facilities.

References and Notes

(1) Jeffrey, G. A. *An Introduction to Hydrogen Bonding*; Oxford University Press: New York, 1997.

(2) Scheiner, S. *Hydrogen Bonding. A Theoretical Perspective*; Oxford University Press: New York, 1997.

(3) Pribble, R. N.; Garret, A. W.; Haber, K.; Zwier, T. S. *J. Chem. Phys*. **1995**, *103*, 10573.

(4) Djafari, S.; Lembach, G.; Barth, H.-D.; Brutschy, B. *J. Chem. Phys*. **1997**, *107*, 10573.

(5) Alkorta, I.; Rozas, I.; Elguero, J. *Chem. Soc. Rev*. **1998**, *27*, 163.

(6) Taylor, R.; Kennard, O. *J. Am. Chem.. Soc*. **1982**, *104*, 5063.

(7) (a) Steiner, T.; et al. *J. Chem. Soc., Perkin Trans. 2* **1996**, 2441. (b) Desiraju, G. R.; Steiner, T. *The Weak Hydrogen Bond*; Oxford University Press: Oxford, U.K, 1999.

(8) Hobza, P.; Špirko, V.; Selzle, H. L.; Schlag, E. W. *J. Phys. Chem. A* **1998**, *102*, 2501.

(9) Hobza, P.; Špirko, V.; Havlas, Y.; Buchhold, K.; Reinmann, B.; Barth, H.-D.; Brutschy, B. *Chem. Phys. Lett.* **1999**, *299*, 553.

(10) (a) Bader, R. F. W. *Atoms in Molecules. A Quantum Theory*; Oxford University Press: Oxford, U.K., 1990. (b) Bader, R. F. W. *Chem. Rev.* **1991**, *91*, 893. (c) Bader, R. F. W. *J. Phys. Chem. A* **1998**, *102*, 7314.

(11) Cubero, E.; Orozco, M.; Hobza, P.; Luque, F. J. *J. Phys. Chem. A* **1999**, *103*, 6394.

(12) Hobza, P.; Havlas, Z. *Chem. Phys. Lett*. **1999**, *303*, 447.

(13) Cubero, E.; Orozco, M.; Luque, F. J. *Chem. Phys. Lett*. **1999**, *310*, 445.

(14) Weber, J. M.; Kelley, J. A.; Robertson, W. H.; Lisle, K. M.; Johnson, M. A.; Havlas, Z.; Hobza, P. *J. Am. Chem. Soc*., submitted for publication.

(15) Reed, A. E.; Curtiss, L. A.; Weinhold, F. *Chem. Rev*. **1988**, *88*, 899.

(16) Wahl, M. C.; Sundaralingam, M. *Trends Biochem. Sci*. **1997**, *22*, 97.

(17) Leonard, G. A.; McAuley-Hecht; Brown, T.; Hunter, W. N. *Acta Cryst*allogr. **1995**, *D51*, 136.

(18) Starikov, E. B.; Steiner, T. *Acta Crystallogr*. **1997**, *D53*, 345.

(19) Kratochvíl, M.; Engkvist, O.; Šponer, J.; Jungwirth, P.; Hobza, P. *J. Phys. Chem. A* **1998**, *102*, 6921.

(20) Hariharan, P. C.; Pople, J. A. *Theor. Chim. Acta* **1973**, *28*, 213.

(21) Boys, S. F.; Bernardi, F. *Mol. Phys*. **1970**, *19*, 553.

(22) Hobza, P.; Havlas, Z. *Theor. Chim. Acta* **1998**, *99*, 372. Simon, S.; Duran, M.; Dannenberg, J. J. *J. Chem. Phys*. **1996**, *105*, 11024.

(23) Špirko, V.; Šponer, J.; Hobza P. *J. Chem. Phys*. **1997**, *106*, 1472.

(24) Frisch, M. J.; Trucks, G. W.; Schlegel, H. B.; Gill, P. M. W.; Johnson, B. G.; Robb, M. A.; Cheeseman, J. R.; Keith, T. A.; Petersson, G. A.; Montgomery, J. A.; Raghavachari, K.; Al-Laham, M. A.; Zakrzewski, V. G.; Ortiz, J. V.; Foresman, J. B.; Cioslowski, J.; Stefanov, B. B.; Nanayakkara, A.; Challacombe, M.; Peng, C. Y.; Ayala, P. Y.; Chen, W.; Wong, M. W.; Andres, J. L.; Replogle, E. S.; Gomperts, R.; Martin, R. L.; Fox, D. J.; Binkley, J. S.; Defrees, D. J.; Baker, J.; Stewart, J. P.; Head-Gordon, M.; Gonzalez, C.; Pople, J. A. *Gaussian 94, Rev. A.1*; Gaussian Inc.: Pittsburgh, PA, 1995.

(25) Frisch, M. J.; Trucks, G. W.; Schlegel, H. B.; Scuseria, G. E.; Robb, M. A.; Cheeseman, J.; Zakrzewski, R.; Montgomery Jr., J. A.; Stratmann, R. E.; Burant, J. C.; Dapprich, S.; Millam, J. M.; Daniels, A. D.; Kudin, K. N.; Strain, M. C.; Farkas, O.; Tomasi, J.; Barone, V.; Cossi, M.; Cammi, R.; Mennucci, B.; Pomelli, C.; Adamo, C.; Clifford, S.; Ochterski, J.; Petersson, G. A.; Ayala, P. Y.; Cui, Q.; Morokuma, K.; Malick, D. K.; Rabuck, A. D.; Raghavachari, K.; Foresman, J. B.; Cioslowski, J.; Ortiz, J. V.; Stefanov, B. B.; Liu, G.; Liashenko, A.; Piskorz, P.; Komaromi, I.; Gomperts, R.; Martin, R. L.; Fox, D. J.; Keith, T.; Al-Laham, M. A.; Peng, C. Y.; Nanayakkara, A.; Gonzalez, C.; Challacombe, M.; Gill, P. M. W.; Johnson, B.; Chen, W.; Wong, M. W.; Andres, J. L.; Head-Gordon, M.; Replogle, E. S.; Pople, J. A. *Gaussian 98, Rev. A.7*; Gaussian Inc.: Pittsburgh, PA, 1999.

(26) (a) Popelier, P. L. A. *J. Phys. Chem A* **1998**, *102*, 1873. (b) Carroll, M. T.; Chang, C.; Bader, R. F. W. *Mol. Phys*. **1988**, *65*, 695. (c) Destro, R.; Biachi, R.; Gatti, C.; Merati, F. *Chem. Phys. Lett*. **1991**, *47*, 186. (d) Alkorta, I.; Elguero, J. *J. Phys. Chem. A* **1999**, *103*, 272. (e) Rozas, I.; Alkorta, I.; Elguero, J. *J. Phys. Chem. A* **1998**, *102*, 9925. (f) Luque, F. J.; Lopez, J. M.; Lopez de Paz, M.; Vicent, C.; Orozco, M. *J. Phys. Chem. A* **1998**, *102*, 6690. (g) Cubero, E.; Orozco, M.; Luque, F. J. *J. Phys. Chem. A* **1999**, *103*, 315.

(27) Biegler-Kšnig, F.; Bader, R. F. W.; Tang, T. H. J. *Comput. Chem.* **1982**, *3*, 317.

(28) (a) Hobza, P.; Šponer, J.; Polásek, M. *J. Am. Chem. Soc*. **1995**, *117*, 792. (b) Šponer, J.; Leszczynski, J.; Hobza P. *J. Phys. Chem*. 1996, *100*, 1965. (c) Hobza, P.; Šponer, J. *Chem. Phys. Lett*. **1998**, *288*, 7.

(29) Kock, U., Popelier, P. L. A. *J. Phys. Chem*. **1995**, *99*, 9747.

(30) (a) Alkorta, I.; Rozas, I.; Elguero, J. *Struct. Chem*. **1998**, *9*, 243. (b) Alkorta, I.; Rozas, I.; Elguero, J. *J. Mol. Struct. (THEOCHEM)* **1998**, *452*, 227. (c) Alkorta, I., Elguero, J. *J. Phys. Chem. A* **1999**, *103*, 272.

(31) (a) Boyd, R. J.; Choi, S. C. *Chem. Phys. Lett*. **1985**, *120*, 80. (b) Boyd, R. J.; Choi, S. C. **1986**, *129*, 62. (c) Bader, R. F. W.; Tang, T. H.; Tal, Y.; Biegler-Kšnig, F. *J. Am. Chem. Soc*. **1982**, *104*, 946. (d) Mallinson, P. R.; Wozniak, K.; Smith, G. T.; McCormack, K. L. *J. Am. Chem. Soc*. **1997**, *119*, 11502. (e) Roversi, P.; Barzaghi, M.; Merati, F.; Destro, R. *Can. J. Chem*. **1996**, *74*, 1145.

(32) Šponer, J.; Leszczynski, J.; Hobza, P. *J. Phys. Chem. A* **1997**, *101*, 9489 (b) Shishkin, O. V.; Šponer, J.; Hobza, P. *J. Mol. Struct*. **1999**, *477*, 15. (c) Guerra, C. F.; Bickelhaupt, F. M.; Snijders, J. G.; Baerends, E. J. *Eur. J. Chem*. **1999**, *5*, 3581.